Supplementary Information

A Non-Topological Mechanism for Negative Linear Compressibility

Jack Binns, Konstantin V. Kamenev, Katie E. R. Marriott, Garry J. McIntyre, Stephen A. Moggach, Mark Murrie, and Simon Parsons

S1 – Experimental Details

Synthesis

A solution of $Co(OAc)_2 \cdot 4H_2O$ (0.249 g, 1 mmol), citric acid monohydrate, (0.21 g, 1 mmol) and potassium hydroxide (0.168 g, 3 mmol) in a 1:1 mixture of H_2O and EtOH (9 ml) was heated under solvothermal conditions at 393 K for 48 hours, then cooled to ambient temperature at a rate of 4 K hr^{-1}. A violet crystalline solid was obtained. This was filtered, washed with Et_2O, and air- dried (yield = 20%).

X-ray Data Collection

Single-crystal diffraction data were collected on a Bruker SMART APEX II diffractometer with graphite-monochromated Mo Kα radiation (λ = 0.71073 Å).[18] All data were integrated using *SAINT*, absorption corrections were carried out in *SADABS*.[19] Dynamic masks were applied to account for shading by the cell body.[20] The program *SHADE* was used to omit partially shaded and diamond reflections.[21] Structures were solved with *SIR*92; refinement was carried in *CRYSTALS* against $|F|^2$.[22, 23] High-pressure single-crystal diffraction experiments were carried out using a Merrill-Bassett diamond anvil cell with a tungsten gasket.[24] The sample and a chip of ruby were loaded with Fluorinert FC70 as the hydrostatic medium. Pressure-dependent ruby fluorescence was used to measure the pressure.[25] Bulk and linear compressibility coefficients were calculated using *EosFit* 7.0.[26] [References are given in the main text.]

Crystal structure refinement

The more extensive data at ambient pressure were collected outside the pressure cell. Refinement against the subset of these reflections with the same indices as those observed at high pressure gave essentially the same parameters with slightly higher standard deviations. Data with $I \geq 2\sigma(I)$ were used for the refinements against the ambient-pressure and 0.3 GPa data sets; at 0.5 and 1.0 GPa data with $I \geq 3\sigma(I)$ were used.

In addition to the framework structure described in the text, UTSA-16 contains large pores occupied by disordered water molecules. At 300 K, the contents of the pore could be modelled with three water molecules per asymmetric unit. Oxygen atoms O80/O81 are bound to K1 forming a disordered pair with K-O bond lengths of 2.82(2) and 2.79(2) Å respectively. Another disordered pair is formed by oxygen atoms O9 and O10 with occupancies of 0.644(15) and 0.462(15) respectively, forming H-bonds with O5 which is the only carboxylate oxygen not bound to a metal. O11, which is fully occupied, lies at a distance of 2.54(3) Å from O80 indicating a possible hydrogen-bonding interaction. Further water sites can be resolved in the pore at low temperatures.

Single-crystal diffraction data were also collected at 100 K, the pore contents were refined to a model consisting of six water molecules, two of which occupy fully ordered sites, with the remainder split across disordered sites. The positions and refined occupancies are essentially the same as reported by Xiang *et al*.[15] One disordered site O80/O81 binds to K1 at a distance of 2.807(11)/2.816(14) Å, each K1 is coordinated by six citrate oxygen atoms and two symmetry-related O80/81 sites to give a full 8-coordinate shell. Oxygen sites O9 and O13 refine to full occupancy. The remainder of the oxygen sites form chains,

linked by hydrogen bonding and tether to the dangling citrate O5 atoms by distances of 2.74(2) and 2.80(2) Å.

The poorly-defined water sites at ambient pressure does not appear in Fourier difference maps at high pressure, the coordination distance for the remaining, isotropically refined, split site does not change significantly over the pressure range.

Rigid-body and rigid-bond restraints were applied to the citrate anions only. All bond lengths and angles were free to refine. Crystal structure details are given in Table S1.

Table S1: Crystal Data and Details of the Structure Determination for: UTSA-16 in $I\bar{4}2d$ at ambient, 0.3, 0.5, and 1.0 GPa. Estimated standard deviations in the least significant digits are given in parentheses.

Crystal data				
a, *b*, *c* [Å]	13.0691(4) 13.0691(4) 30.1570(10)	13.0005(5) 13.0005(5) 30.2002(11)	12.8201(5) 12.8201(5) 30.2685(12)	12.6111(5) 12.6111(5) 30.2999(11)
V [Å]	5150.9(4)	5104.2(3)	4974.8(4)	4818.9(4)
Data collection				
Pressure [GPa]	Ambient	0.3(1)	0.5(1)	1.0(1)
2θmin. and max. [°]	1.7, 25.3	3.7, 24.1	3.7, 24.7	3.7, 24.4
Data set (h_{min}:h_{max}; k_{min}:k_{max} ; l_{min}:l_{max})	-11: 11 ; 0: 15 ; 0: 36	-8: 8 ; 0: 13 ; 0: 34	-7: 7 ; 0: 13 ; 0: 34	-7: 7 ; 0: 13 ; 0: 34
Total data, Unique data, R_{int}	24384, 2365, 0.046	7155, 1476, 0.048	7130, 1515, 0.050	6416, 1397, 0.052
Observed data [$I > 2\sigma(I)$]	2187	1282	1337	1217
Refinement				
N_{ref}, N_{par}	2187, 164	1282, 149	1260, 154	1155, 154
R, w*R*2, *S*	0.0352, 0.0893, 0.90	0.0576, 0.1485, 0.95	0.0672, 0.1806, 1.02	0.0774, 0.2027, 1.02
Flack *x*	0.04(2)	0.07(5)	0.08(5)	0.13(7)
Minimum and Maximum Residual Density [*e* Å^{-3}]	-0.51, 0.72	-0.52, 1.14	-0.77, 1.39	-0.72, 2.25

S2 Calculation of geometric parameters

The Co2-tetrahedral torsion angle, ϕ, is defined as the plane twist angle (rotation of the planes around the centroid-centroid direction) between plane O2–Co2–O2^{ii} and plane O7^{iii}–Co2–O7^{i}. Figure S1 shows the Co2 tetrahedral planes in projection along the *c* axis. Symmetry labels are i = [*y* − ½, *x*, *z* − ¼] ii = [1−*x*, 1−*y*, *z*] iii = [½ − *y*, 1 − *x*, *z* − ¼]. Tetrahedron length, *l*, is calculated using the fractional *z* coordinates of O2 and O7^{i} and the *c*-axis length according to $l = |z_{O2}-z_{O7}|c$

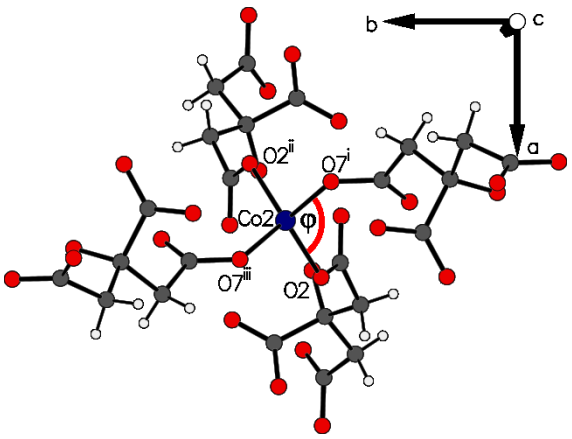

Figure S1 Projection view of Co2 tetrahedral planes illustrating torsion angle ϕ

Table S2 Derived geometrical parameters in Co tetrahedra.

Pressure / GPa	ϕ/°	*l* / Å
0	98.37(8)	2.316(3)
0.3(1)	99.4(2)	2.314(5)
0.5(1)	102.7(2)	2.328(6)
1.0(1)	106.4(3)	2.345(9)

S3 The contribution of changes at Co2 to the NLC along the c-axis

Fig. 4 in the main text shows a simplified structure containing just the Co2 tetrahedra, the centroids of the $Co1_4O3_4$ cubanes and the potassium ions. The height of the Co2 tetrahedron is the distance between the centroids of the upper and lower edges (O2…O2 and O7…O7) projected onto **c**, but because of the two-fold symmetry this is readily obtained as $c|z(O2) - z(O7)|$. This corresponds to *l* in Fig. 3. The height at ambient pressure is 2.3164 Å, and 2.3452 Å at 1 GPa, a difference of +0.0288 Å. The compressibility of the anion in the *c*-direction is therefore −12.4 TPa^{-1}, calculated according to

$$\beta_d = -\frac{1}{d}\left(\frac{\partial d}{\partial P}\right)_T \sim -\frac{1}{d}\left(\frac{\Delta d}{\Delta P}\right)_T$$

There are eight CoO_4^{2-} anions per cell, and so their contribution to the NLC effect seen along *c* is 0.0288 x 8 = 0.2304 Å. Since this is greater than the NLC effect actually observed (0.1429 Å) there must be some compensation occurring by compression of other regions of the structure.

The *c* axis length is a function of three different distances, labelled A, B and C in Fig. 4, and listed in Table 1.

B is the height of the Co2 tetrahedron referred to above. A and C can be evaluated in a similar way, except that O2 and O7 are in different anions. ΔB comes from the changes in the Co2 tetrahedron identified as *l* in Fig. 3 of the main text, and contributes to a lengthening in the *c* axis. ΔC is negative and corresponds to compression of a potassium rich region of the structure.

Table S3: Changes along the *c*-axis with pressure.

Region	Ambient Pressure/Å	1 GPa/Å	Δ/Å
A	0.8402	0.9272	0.0870
B	2.3164	2.3452	0.0288
C	2.0663	1.9574	−0.1089
Total *c*-axis = 4A+8B+4C	30.1572	30.3000	0.1428
Observed *c*-axis	30.1570	30.2999	0.1429

ΔA is numerically quite small and the region does not actually contain any atoms except for those used to define its boundaries and C5, which also sits on the boundary. The positive value of ΔA seems to be the result of citrate ligands being pulled in opposite directions by contractions around the K^+ ions in region C (Table S4), and it is reasonable to treat regions A and C together. The value of (ΔA + ΔC) is −0.0219 Å, similar to ΔB, but because there are eight B regions and 4 each of A and C, the overall change in the *c* axis length is 8ΔB + 4(ΔA + ΔC) = +0.1428 Å (~+0.1429 Å allowing for rounding errors).

Table S4: Atom-Atom distances formed in region A (defined as 0.48 < *z* < 0.52)

Atom 1		Atom 2		dist/Å	Atom 1 coordinates			Atom 2 coordinates		
C5	1-y,-1+x,1-z	O7	1-y,-1+x,1-z	0.038	0.316	0.0774	0.4867	0.4241	0.0877	0.4847
C5	1-y,-1+x,1-z	C5	x-1,y,z	0.011	0.316	0.0774	0.4867	0.0915	0.6763	0.5134
C5	1-y,-1+x,1-z	O7	x-1,y,z	0.049	0.316	0.0774	0.4867	0.0877	0.5759	0.5153
O7	1-y,-1+x,1-z	O7	x-1,y,z	0.087	0.413	0.0742	0.4861	0.0877	0.5759	0.5153

S4 The contribution of changes at Co2 to the NLC along the a-axis

A similar exercise can be carried out for the *a* axis (Fig. 4 in the main text) by separating it into regions D and E (Table S5). The value of D can be calculated from the positions of the centroids of O2 and O7 (X2 and X7). The projection of the centroid-centroid vector on the *a* axis is D = $a|x(X2) - x(X7)|$.

ΔD comes from changes in the Co2 tetrahedron, and the substantial value (–0.1719 Å) reflects changes in the Co2 coordination sphere; the change corresponds to a compressibility of 84.3 TPa^{-1}. ΔE is about three times smaller.

The change in *a* axis length is given by $\Delta a = 2\Delta D + 2\Delta E$. Neglecting ΔE gives the contribution of the Co2 tetrahedron to Δ*a*, yielding a calculated value at 1 GPa of 13.0691 – (2 x 0.1719) = 12.7253 Å (cf 12.6111 Å experimentally).

Table S5: Changes along the *a*-axis with pressure.

Region	Ambient Pressure/Å	1 GPa/Å	Δ/Å
D	2.0396	1.8677	−0.1719
E	4.4950	4.4378	−0.0572
Total *a*-axis = 2D+2E	13.0692	12.6110	−0.4582
Observed *a*-axis	13.0691	12.6111	−0.4580

The experimental cell dimensions between ambient pressure and 1 GPa lead to compressibilities β_a = 35.04 TPa^{-1} and β_c = −4.74 TPa^{-1}. Considering only the changes at Co2 (i.e. regions B and D) leads to cell dimensions at 1 GPa of *a* = 12.7253 and *c* = 30.3874 (= 30.1570 + 0.2304) Å; use of these values in place of the experimental values 1 GPa yields β_a = 26.31 TPa^{-1} and β_c = −7.64 TPa^{-1}. This demonstrates the overall influence of the changes at Co2 in the compression of the crystal, and that elongation of the eight CoO_4^{2-} anions outweighs the compression of the four potassium rich regions labelled 'C'.

S5 Topological analysis based on a Diamondoid lattice

A referee to the first submission of this paper suggested that an alternative analysis of the compression mechanism could be based on a diamondoid lattice derived by consideration of only the centroids of the cubanes (X1 in Fig. 4 in the main text). The strut dimensions are given in Table S6 along with the two unique angles between the struts (the site symmetry is −4). The cell dimensions are $a = 2d\sin(\theta_1/2)$ and $c = 4d\cos(\theta_1/2)$. Rearranging gives $\tan(\theta_1/2) = 2a/c$ and $d = a/(2\sin(\theta_1/2)) = c/(4\cos(\theta_1/2))$.

Table S6: Diamondoid lattice dimensions.

P/GPa	*d*/ Å	θ_1/°	*a*/Å	*c*/Å
0	9.9770	81.833	13.0691	30.1570
1.0	9.8560	79.549	12.6111	30.2999

The data in Table S6 above give the strut compressibility to be +12.1 TPa^{-1}. The contribution of the angle was obtained by holding *d* fixed and calculating the cell dimensions with the values of θ_1 given in Table S6. For Δ*P* = 1 GPa this gives,

$$\beta_{a\theta} = 1 - \frac{\sin(\theta_1^{1GPa}/2)}{\sin(\theta_1^{0}/2)}$$

$$\beta_{c\theta} = 1 - \frac{\cos(\theta_1^{1GPa}/2)}{\cos(\theta_1^{0}/2)}$$

yielding $\beta_{a\theta}$ = +23.19 TPa^{-1} and $\beta_{c\theta}$ = −17.08 TPa^{-1}.

The changes to the dimensions of the Co2-based tetrahedron are translated into diamondoid lattice dimensions in Table S7. This is developed in Table S8 to show the influence of the strut compression versus the angle compression on the axial compressibilities.

Table S7: Analysis of diamondoid lattice dimensions in terms of Co2 distortions

Model	Change	*a*/Å	*c*/Å	*d*/Å	θ_1/°	β_a/TPa^{-1}	β_c/TPa^{-1}
1	obs 0 GPa	13.0691	30.1570	9.9770	81.833		
2	8B	13.0691	30.3874	10.0206	81.402	0.00	-7.64
3	8B+4(A+C)	13.0691	30.2998	10.0040	81.566	0.00	-4.74
4	2D	12.7253	30.1570	9.8653	80.324	26.31	0.00
5	2D+2E	12.6109	30.1570	9.8285	79.815	35.06	0.00
6	8B + 2D	12.7253	30.3874	9.9094	79.895	26.31	-7.64
7	4A+8B+4C+2D+2E	12.6109	30.2998	9.8559	79.549	35.06	-4.74
8	obs 1 GPa	12.6111	30.2999	9.8560	79.549	35.04	-4.74

Table S8: Separation of the effects of *d* and θ from Table S7. a_θ is the value of *a* considering only the change in θ and holding *d* fixed at 9.9770 Å. $\beta_{a\theta}$ is calculated from the value of a_θ using the (experimentally-determined) value in model 1 as the reference.

Model	Change	*d*/Å	θ_1/°	β_d/TPa^{-1}	a_θ/Å	c_θ/Å	$\beta_{a\theta}$/TPa^{-1}	$\beta_{c\theta}$/TPa^{-1}
1	obs 0 GPa	9.9770	81.833	-	13.0691	30.1570	-	-
2	8B	10.0206	81.402	-4.37	13.0122	30.2552	4.35	-3.26
3	4A+8B+4C	10.0040	81.566	-2.71	13.0338	30.2180	2.70	-2.02
4	2D	9.8653	80.324	11.20	12.8694	30.4986	15.28	-11.33
5	2D+2E	9.8285	79.815	14.89	12.8015	30.6127	20.48	-15.11
6	8B + 2D	9.9094	79.895	6.78	12.8122	30.5948	19.66	-14.52
7	4A+8B+4C+2D+2E	9.8559	79.549	12.14	12.7659	30.6721	23.20	-17.08
8	obs 1 GPa	9.8560	79.549	12.13	12.7660	30.6720	23.19	-17.08

Line 2 shows that Co2 tetrahedral elongation causes the struts to expand, as expected, but θ_1 decreases causing *a* to decrease in length and *c* to increase. The compression of the Co2 tetrahedron in the *a*-direction induces quite large changes (model 4), where both the strut length and θ_1 decrease, the effect of the latter being NLC along *c*. The large value of $\beta_{c\theta}$ is thus actually mostly an effect of compression in the *a*-direction. Note that about 85% of the NLC effect can be ascribed to changes in the internal geometry of the Co2 tetrahedron (cf lines 6 and 7).

S6 Cambridge Structural Database search

Distributions of X-Co-X bond angles for X = N and O for (a) tetrahedral and (b) octahedral Co(II) complexes were extracted from data deposited in the Cambridge Structural Database. The small peaks to the left of the dominant peaks occur for bidentate ligands with small bite angles (e.g. carboxylate).

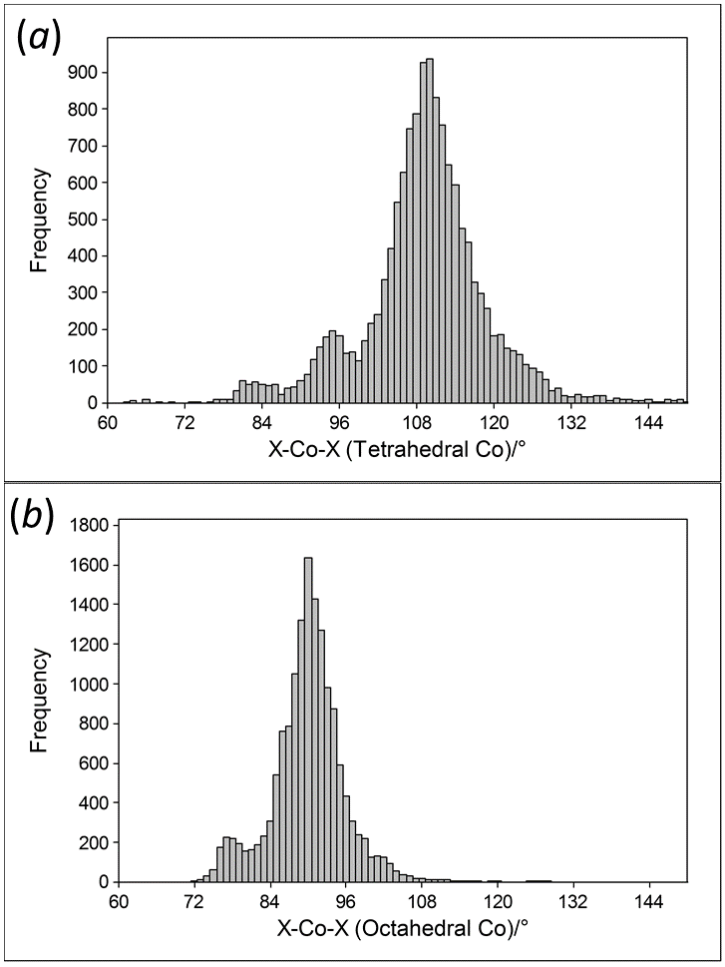

Figure S2. Distributions of X-Co-X bond angles for X = N and O for tetrahedral and octahedral complexes deposited in the Cambridge Structural Database.